Guardiola, C.; Pla Moreno, B.; Piqueras, P.; Mora-Pérez, J.; Lefebvre, D. (2017). Model-based passive and active diagnostics strategies for diesel oxidation catalyst. Applied Thermal Engineering. 110:962-971. doi:10.1016/j.applthermaleng.2016.08.207

Model-based passive and active diagnostics strategies for diesel oxidation catalysts

C. Guardiola [a] B. Pla [a] P. Piqueras [a] J. Mora [a] D. Lefebvre [b]

[a] *CMT–Motores Térmicos, Universitat Politècnica de València, Valencia, Spain (e-mail:* {carguaga,benplamo,pedpicab,jamopre1}*@mot.upv.es).*

[b] *PSA Peugeot Citroën, La Garenne-Colombes, France (e-mail: damien.lefebvre@mpsa.com)*

Abstract

This article proposes a diesel oxidation catalyst diagnostics strategy based on the exothermic process generated by exhaust gas species oxidation in the catalyst. The diagnostics strategy is designed to be applied on-board and respecting real-time electronic control unit computational limitations. Diagnosis purposes are fulfilled by means of the comparison of the passive model temperature, which represents the outlet temperature of a non-impregnated diesel oxidation catalyst, and the measurement provided by the on-board catalyst-out temperature sensor. Thus, the presented diagnostics strategy uses only two production grade temperature sensors and the measurements of air and fuel mass flows from the electronic control unit. Passive diagnostics is based on the oxidation of engine-raw emissions, whilst active diagnostics is based on the oxidation of requested post injected fuel. Post-injection strategy is also discussed for active diagnosis. Then, the diagnostics strategy is able to discern whether the diesel oxidation catalyst is able to oxidise or not.

Key words: Diesel oxidation catalyst, thermal model, diagnosis, post-injection, turbocharged engine

1. Introduction

Exhaust gases regulation of diesel engines has become more stringent during recent decades. Emission limits have decreased and normative is trying to increasingly approach to real driving conditions [1]. Traditional direct injection combustion engines technology is not able to accomplish regulation limit thresholds with only in-cylinder technology, so aftertreatment systems are necessary to reduce tail-pipe pollutant emissions [2]. However, aftertreatment aging may mitigate its efficiency over time and on-board diagnosis (OBD) should detect defficiencies which increment concentrations of tail-pipe pollutant species [3]. In this article, an OBD strategy is presented for diesel oxidation catalysts (DOC).

Several aftertreatment systems are already being used in light duty vehicles. The most commonly used is the diesel oxidation catalyst [4]. Washcoat on the ceramics substrate of diesel oxidation catalysts is generally impregnated with a certain proportion of Pt and Pd. It allows the oxidation of HC, CO and NO species [5], as well as the soluble organic fraction (SOF) of the particulate matter (PM) [6], all present in engine-raw exhaust gases. The DOC is placed between the engine and the rest of aftertreatment systems, since it affects the performance of diesel particulate filters (DPF) during regeneration conditions [7] and selective catalytic reduction (SCR) by reducing the NO/NO_2 ratio [8, 9]. Then, a proper operation of DOCs is essential to keep an overall aftertreatment efficiency.

Diesel oxidation catalysts are subjected to several permanent and temporary deactivation mechanisms. Main permanent causes are thermal damage, induced by generating exotherm on the catalyst, and exposure to various inorganic species contained in engine fluids [10]. As an example of a temporary DOC damage, light-off temperature is increased due to an exposure to excessive temperature [11]. Deactivation mechanisms show significant effects on NO and C_3H_6 oxidation [12, 13].

On-board diagnosis approaches must take into account the limitations of on-board applications. On-board sensors are limited in commercial vehicles due to the extra cost they add. Then, control oriented models are used to reduce as much as possible the number of sensors used. The control-oriented model used in this work, which respects the computational resources of the Electronic Control Unit (ECU), can be found in [14]. Only temperature, air mass flow and fuel mass flow are used as inputs to the strategy. Then, no

Table 1
DOCs used in the experiments and its main characteristics.

DOC	Ceramics configuration
nominal	With washcoat
non-impregnated	Without washcoat

estimation of HC, CO nor NO concentrations is done as far as no sensor is to be used in real world vehicles and there is also difficulty of modelling them.

Eventually, the objective of the article is to introduce an on-board real-time diagnostics strategy based on the exothermic generated by the DOC when there is presence of oxidable species, which has to be able to discern whether a DOC is able to oxidise or not. In passive diagnosis, during normal driving conditions, engine-raw emissions are not able to feed the DOC with enough HC [15] to generate enough increment of temperature at the outlet of the DOC. Therefore, post-injections are used in active diagnosis as an extra excitation to increase HC concentration at the inlet of the DOC [16, 17]. Post-injections used during DPF active regeneration phases can be also used for DOC diagnostics purposes.

Paper is structured as follows. Section 2 describes the experimental set-up and presents the on-purpose sensors used. Section 3 presents the general diagnostics strategy. Section 4 discusses the post-injection strategy approach. Finally, conclusions are presented in section 5.

2. Experimental setup

The engine used in this study is a common light-duty engine equipped with a high pressure common-rail fuel injection system, a variable geometry turbine and a high pressure exhaust gas recirculation system. A DOC was the only aftertreatment device in the exhaust line, in company with a back pressure valve to substitute the pressure drop effect of a DPF. A pair of different DOCs, listed in Table 1, have been tested. On the one hand, a DOC with washcoat, named nominal DOC, is able to perform oxidation of the different species and accumulate HC [18, 19]. It is used to represent the behaviour of a new DOC. On the other hand, a DOC without washcoat, named non-impregnated DOC, is used in order to calibrate the model. This DOC does not have any oxidation capability, so it is only able to behave as a regenerative heat exchanger.

A bypass was done to the ECU of the engine through an ETAS 910 and a National Instruments Real Time PXI, mainly in order to post inject raw fuel when necessary, as sketched in Figure 1. Different acquisition sensors, shown in Figure 2, were installed along the exhaust line and the DOC. Three thermocouples measure DOC core temperature at different sections in the axial direction. Two Denso negative temperature coefficient (NTC) sensors are installed to measure temperature at the inlet T_{in} and the outlet T_{out} of the DOC. Sensors are able to measure a range

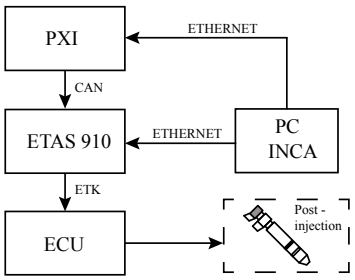

Fig. 1. Scheme of the bypass performed to the engine ECU with post-injection purposes.

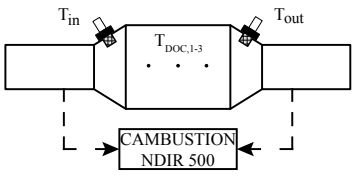

Fig. 2. DOC instrumentation layout

of temperatures from -30 to 1000°C, with standard responsiveness, according to the sensor manufacturer. This kind of sensors are installed in commercial vehicles, therefore their response and precision will be such as the measurement that will feed the ECU. A Cambustion NDIR 500 was used to have a fast measurement of CO_2, which response time is around 10ms. As the general dynamics of the system are in the order of magnitude of seconds, measurements read by this fast gas analyser can be understood as non-delayed values of the gas concentration. Thermocouples were connected to a PUMA measuring system, while the two NTC temperature sensors and the Cambustion NDIR 500 were connected to the PXI through an analogic connection.

The origin of the inputs used in the diagnostics strategy are presented in this paragraph. The measurement of the intake air mass flow is captured by a flowmeter located at the intake manifold of the engine. The value of the fuel injected, including post-injection conditions, is given by the look-up tables depending on injection duration and rail pressure. In order to obtain the total exhaust mass flow, the values of the air mass flow and the fuel injected are summed. The two NTC sensors provide the temperature of the exhaust line before and after the DOC. Thanks to the low number of inputs of the model, error due to measurements can be kept low. NTC sensors present an error of ±7°C at mid temperatures and of ±10°C at low and very high temperatures, according to the sensor manufacturer. As reported by [3], flowmeter error is in the order of magnitude of 3%. The combined error of sensors and injectors depend on the engine used for the final implementation.

3. General diagnostics strategy

The diagnostics strategy is based on the exothermic reactions caused by DOC activity, mainly due to the oxidation of HC and CO. Thus, when the DOC is oxidising, the outlet temperature increases with respect to the temperature

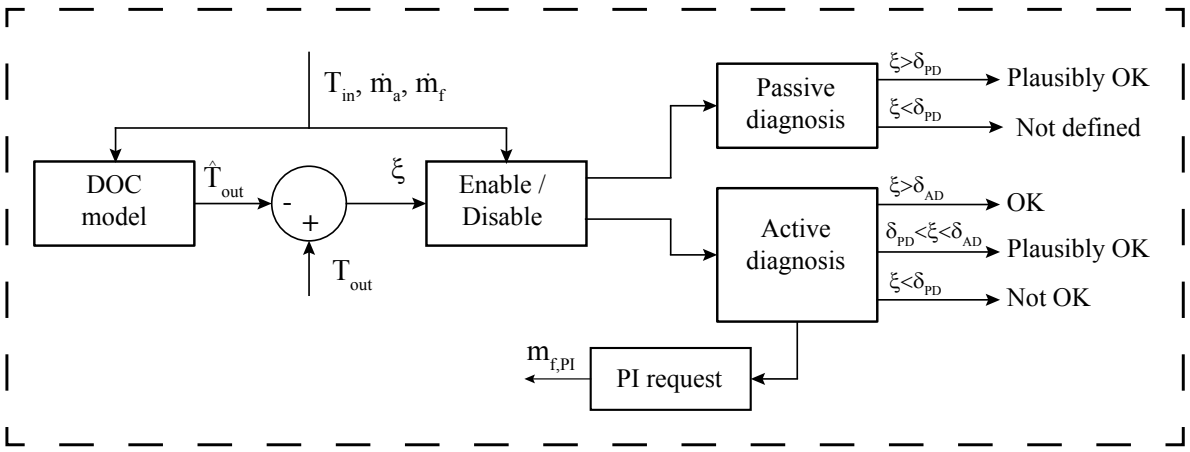

Fig. 3. Scheme of the diagnostics strategy.

Table 2
Coefficients of the diagnostics strategy.

Coefficient	Description
T_{in}	Measured DOC inlet temperature
T_{out}	Measured DOC outlet temperature
$\hat{T}_{out}$	Estimated non-impregnated DOC outlet temperature
m_a	ECU estimated air mass flow
m_f	ECU estimated injection fuel
ϵ	Temperature model error
$m_{f,PI}$	ECU estimated post-injection fuel
ξ	Residuum $T_{out} - \hat{T}_{out}$
δ_{PD}	Low diagnosis threshold
δ_{AD}	High diagnosis threshold

that a non-impregnated DOC would have.

The passive model used estimates the outlet temperature of a non-impregnated DOC and ξ is the residuum generated between the measured T_{out} and the modelled $\hat{T}_{out}$ temperatures.

$$\xi = T_{out} - \hat{T}_{out} \tag{1}$$

Then, by comparing these two temperatures, the DOC diagnosis strategy is able to detect activity when the measured temperature is higher than the estimated ($T_{out} > \hat{T}_{out}$). The diagnosis strategy is enabled or disabled depending on flow conditions such as transients, maximum temperature and minimum exhaust flow. In case the diagnosis is enabled, two kinds of diagnosis strategies can be followed. Passive strategy is based on normal driving operating conditions without external excitation, whilst active strategy is based on exothermic oxidation due to post-injections. Fuel post-injections lead to high HC concentrations in the exhaust line, which are translated into an increase of temperature at the DOC outlet. Figure 3 shows the general diagnostics strategy, whose elements will be described in subsequent paragraphs, and table 2 shows its main coefficients.

3.1. *Control-oriented DOC passive model*

As mentioned before, a DOC model is needed in order to estimate the temperature that a sensor at the outlet of a non-impregnated DOC would measure. Several versions of DOC control oriented models have been developed [20, 21], while in [14], the authors present the passive DOC model which will be used in the following. The model is mainly based on energy and mass balances, with a variable delay dependent on a function of the exhaust mass flow. The delay as a function of exhaust mass flow is a key component since lumped model cannot consider the axial heat transmission due to convection and conduction effects [22]. Considering such variable delay approach allows simulating the effects of the heat transfer along the monolith while keeping a very simple model. The fact that the compared temperatures are those measured by the DOC-out sensor highlights the necessity of replicating the sensor signal rather than the actual gas temperature. Model coefficients are highly dependent on the sensor location and a change of place would imply the modification of the coefficients calibration. If the coefficients of the delay function from the exhaust mass flow are such that allow backsteps in time, delay time needs to be filtered until the problem is avoided.

The model requires the flow temperature and the exhaust mass flow at the inlet of the DOC, whose sensors have been previously described. Although the DOC is able to oxidise HC, CO, the SOF of the particulate matter, and convert NO into NO_2, it is not necessary to estimate which is the contribution of each species to the heat released. The increase of temperature due to species oxidation and the gas conditions may vary the heat transfer of the catalyst, even though the passive model does not have to take any effect of combustion into account. As a matter of fact, any gas concentrations at the DOC inlet are used as inputs, since they significantly vary with the considered engine, the operation temperature and have many uncontrolled disturbances. Hence considering those emissions a known input for the model would cause significant errors.

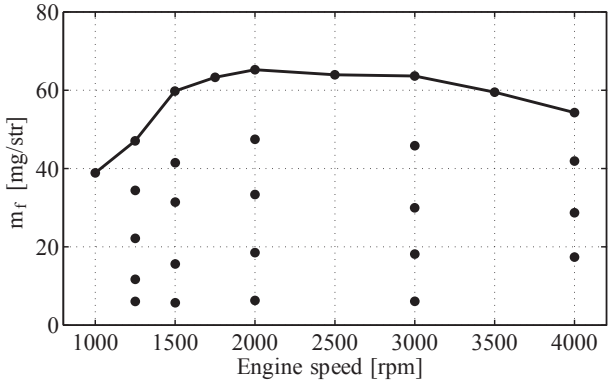

Fig. 4. Engine map of the studied engine with selected points for the characterisation.

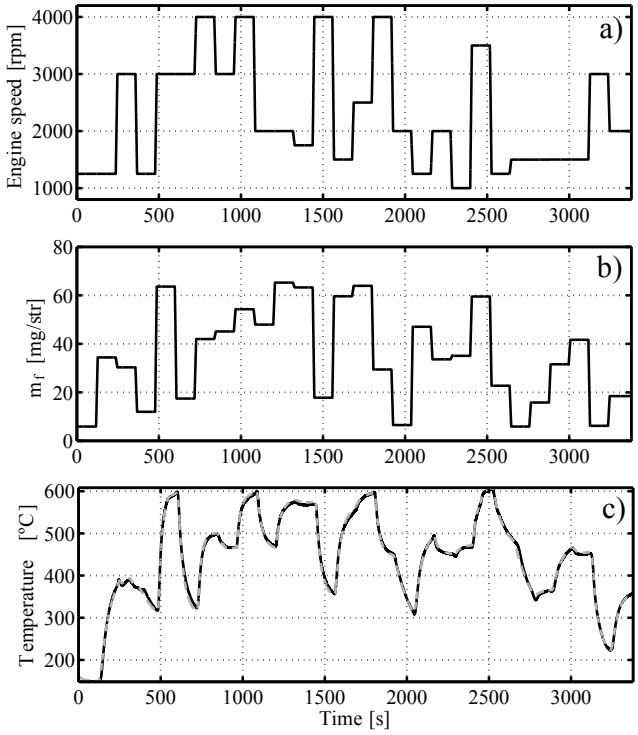

Fig. 5. a) Engine speed, b) Fuel mass flow and c) Modelled (dashed grey) and measured (black) DOC-outlet temperatures of the non-impregnated DOC. The test passes through points marked in the map of Figure 4.

3.1.1. *Validation of the DOC passive model.*

It is important to validate the model in all the possible operating conditions of the engine, also with high dynamics, in order to assure a proper performance of the DOC model during real driving conditions. Figure 4 shows a set of selected points in the speed vs fuel map of the engine which will be used to characterise the engine. These points include different EGR rates, different VGT positions, low and high loads, low and high temperatures, as well as different exhaust mass flows. Note that the DOC is blind to EGR ratio or VGT position, since it is only able to notice exhaust mass flow, temperature and concentrations.

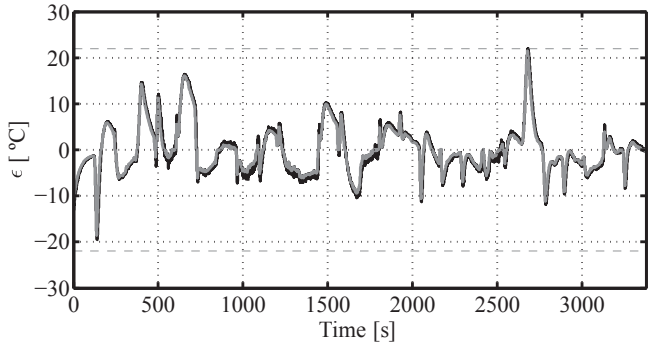

Fig. 6. Black: Error ϵ with the non-impregnated DOC of the validation test of Figure 5. Grey: Filtered error.

Different tests are carried out passing through these points in different order. Figure 5 shows one of these dynamic tests with respect to engine speed, fuel mass flow and both modelled and measured temperatures. Black line of Figure 6 represents the raw error of the model, whilst the grey line represents the error with a filter which consists of the minimum error during a time window of 5 seconds. In addition, a set of tests during more than 5 hours, including those mentioned before and homologation cycles like the New European Driving Cycle (NEDC) or the new World harmonised Light duty Test Cycle (WLTC) at both warm and cold starting conditions, have been used to evaluate the model. The result of all those tests together is shown in Fig. 7 as an error histogram. On the one hand, white filled histogram, represents the probability of a given error during 0.1s. On the other hand, grey filled histogram represents the filtered error, described before for grey line in Figure 6, in which a clear peak at 0 can be observed. This is basically due to the fact that error dynamics are increased during short time lapses.

3.2. *Diagnosis conditions*

There are engine operating conditions which are not suitable for DOC diagnostics [23]. Effective monitoring time is then ruled by enabler conditions which depend on engine operating points, system dynamics and catalyst temperature. These enabler conditions in the proposed strategy are:

- The DOC is sufficiently hot, since the light-off temperature sets the minimum temperature from which the DOC is able to oxidise [24, 25].
- There is sufficient exhaust mass flow. Completely absence of flow in the DOC does not allow diagnosis with oxidation due to obvious reasons.
- The DOC temperature is not excessive, in which case it is hard to detect DOC activity due to huge heat transmission effects.
- dT/dt is not excessive. NTC sensors are rather slow, which causes significant bias in the case of fast varying transients. Therefore, even if the model shows good performance during transients, severe dynamics are to be avoided.

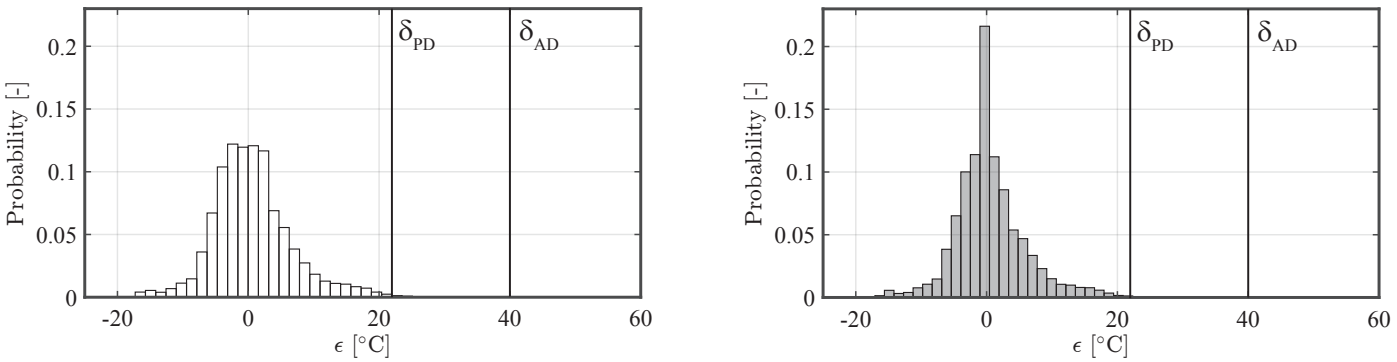

Fig. 7. Histogram of the raw residuum (left) and 5 seconds filtered residuum (right) generated by the model and the non-impregnated DOC in the complete set of tests.

– There is enough oxygen in the exhaust line after the in-cylinder combustion.

3.3. *Low and high diagnosis thresholds*

3.3.1. *Low threshold*

The error generated by the comparison of the outlet temperature of a passive DOC and the modelled temperature are inside an interval of ±22°C, as can be seen in Figures 6 and 7. Although 3σ criteria suggests an error interval of ±18°C, an error interval of ±22°C ensures that the error will not surpass that range during 0.1s with a probability of 10^{-6}%. Therefore, passive detection will provide positive results regarding DOC state when ξ is higher than a low threshold δ_{PD} of 22 °C.

3.3.2. *High threshold*

Even if the model error in Figures 6 and 7 does not overcome the low threshold, a higher threshold δ_{AD}, for active diagnosis, is set to completely ensure the proper state of the DOC. The probability of making a proper diagnostic of the DOC results in a trade-off between the size of the post-injection and the value of δ_{AD}, where the size of the post-injection is the combination of the post-injection duration and injection rate.

Error type I: DOC Failure Miss-detection

If δ_{AD} is too low, a big model error could increase ξ over δ_{AD} and a faulty DOC could be considered as faulty free.

Error type II: DOC Failure Over-detection

If the size of the post-injection is not big enough and ξ does not overcome δ_{AD}, a faulty free DOC would be considered as faulty. It can be considered as a cost parameter, since it determines the size of the post-injection.

Thus, δ_{AD} should be high enough to avoid error type I but, accordingly, the size of the post-injection must ensure that ξ will overcome the threshold to avoid error type II.

3.4. *Passive Diagnostics*

Passive diagnosis consists in the evaluation of ξ during normal driving operation conditions. When diagnosis is enabled and $\xi > \delta_{PD}$, there is a plausibly but-non demanded check that the DOC is oxidising. During cold starting and during some phases in which the exhaust line temperature is under the light-off temperature, a DOC is able to accumulate HC. Therefore, if enough amount of fuel is accumulated in the DOC, when it overcomes the light-off temperature under certain conditions, the accumulated HC will be oxidised and ξ will increase.

For instance, Figure 8 shows the residuum ξ generated during a NEDC homologation cycle. The DOC accumulates HC during the urban phase, except for the short four temperature peaks of the urban part, so when the cycle comes to the extra-urban part and the exhaust temperature rises above the light-off temperature during enough time, the DOC efficiency increases enough to oxidise accumulated HC and ξ clearly overcomes δ_{PD}. Zervas [26] also points out the increment of temperature of the extra-urban part with respect to the urban part of the NEDC, as well as its effect on the DOC efficiency increment. Despite oxidation phases can be appreciated when $\xi > \delta_{PD}$, negative phases mark the presence of the inherent error of the model. In fact, the combined effect of the error model and the temperature increment due to oxidation may not be separated when using the nominal DOC.

Oxidation is subjected to particular driving conditions, but the NEDC cycle is unlikely to be done by a real driver. Indeed, HC and CO engine-raw emissions are usually low for a diesel engine with conventional combustion when in warm operation and experience suggests that exothermic reaction generated by normal combustion operation does not overcome a ξ of 50°C. On the other hand, if diagnosis conditions are enabled but $\xi < \delta_{PD}$, a decision cannot be taken regarding the DOC state in order to avoid error type II.

3.5. *Active Diagnostics*

Active diagnosis consists in the evaluation of ξ when specific post-injection events are performed. Note that only active diagnosis is able to decide whether the DOC is completely OK or if by contrast is not OK. The active diagnosis algorithm decides when a post-injection event is required

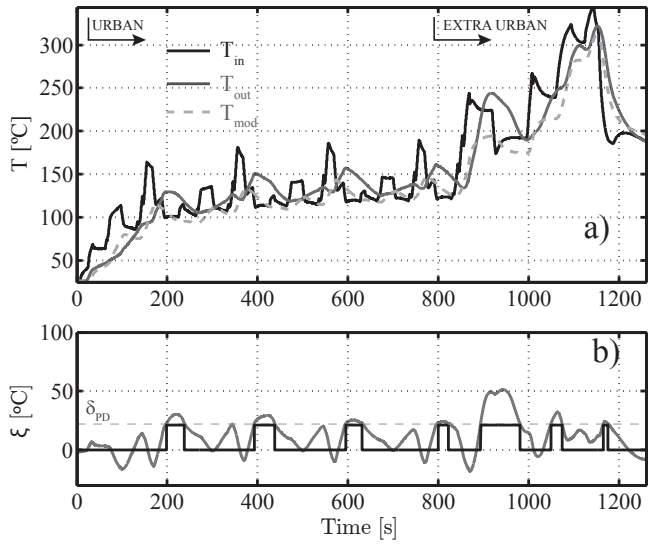

Fig. 8. Passive diagnostics with the nominal catalyst during a NEDC test. a) Temperatures. b) Grey: ξ. Black: 0 when no oxidation and δ_{PD} when $\xi > \delta_{PD}$.

depending on how many kilometers have passed since the last high-check. It can take advantage of the post-injections demanded by the DPF regeneration system or it can request their own. When fuel is post injected in the exhaust line, a temporary window is opened, during which active diagnosis is enabled, as long as the rest of diagnosis conditions are accomplished. If $\xi > \delta_{AD}$ during a certain time inside the window, the result of the diagnosis will be positive. If $\delta_{AD} > \xi > \delta_{PD}$, diagnosis can not assure completely the proper state of the DOC, so it results in a low check and the DOC is plausibly OK. Otherwise, if $\xi < \delta_{PD}$, the result of the diagnosis is negative, the DOC is not OK and the vehicle should go to the workshop after a certain number of failure checks (Fig. 3).

4. Post-injection strategy approach

The diagnostics strategy is able to discern whether there is oxidation or not, although it is not able to predict ξ originated by post-injections. The target of the post-injection calibration is to overcome δ_{AD} during the temporal window while active diagnosis is enabled, according to the engine operating conditions given at the moment of the post-injections, which depend on the vehicle driver.

Post-injections can be performed as pulsed or continuous, depending on the injection duration. In the experiment shown in Figure 9, continuous steps of post-injection have been applied (1, 3 and 5 mg/str) during engine steady state conditions. Figure 10 is then obtained through the combination of different continuous post-injections tests and can be used to analyse the effect of exhaust mass flow and post injected fuel on ξ: ξ increases with increasing post-injected fuel, $\dot{m}_{f,PI}$, and with decreasing exhaust mass flow, $\dot{m}_{exh}$.

The DOC diagnostics strategy can also take advantage of the DPF regeneration system. A DPF is regenerated

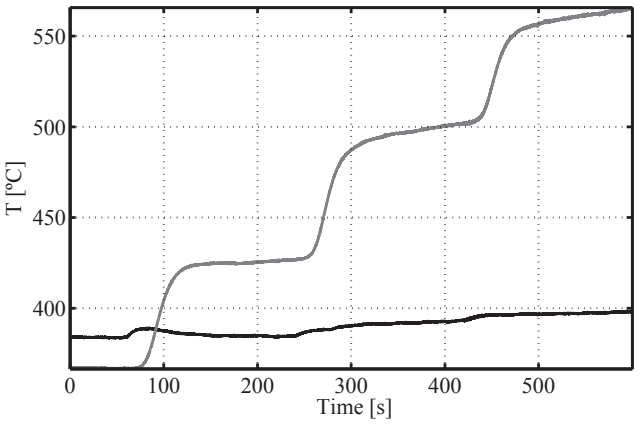

Fig. 9. Continuous post-injections of 1, 3 and 5 mg/str under steady state conditions. Black: inlet temperature. Grey: Outlet temperature.

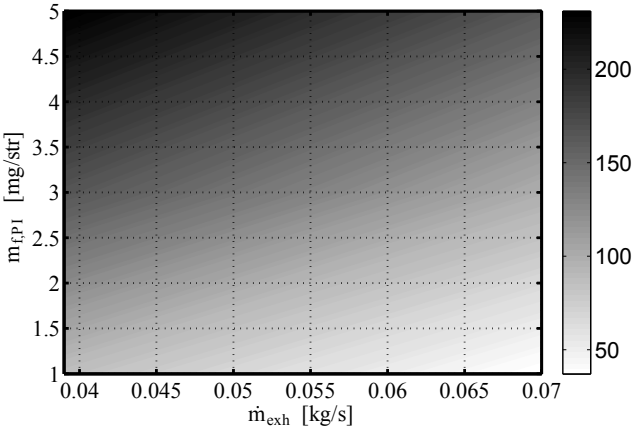

Fig. 10. Experimental effect of air mass flow and continuous post injected fuel on ξ [°C].

by bringing the DPF inlet temperature up to around 620 °C [27]. It is done normally by post-injecting fuel, among other procedures like the modification of the main injection timing. During real DPF regeneration conditions, $\dot{m}_{f,PI}$ is modified to match the objective DPF inlet temperature. Then, active diagnosis post-injection requests can be combined with DPF regeneration events in order to save fuel.

4.1. *Post-injection pulses*

Post-injection pulses are an efficient way in terms of fuel consumption to increase ξ over δ_{AD} during the minimum required time. In the following, the behaviour of the DOC is analysed under steady state conditions when post-injections have been performed. Likewise, a steady state model is developed to estimate the ξ peak also under steady state conditions. However, since steady state conditions cannot be assured during real driving conditions, the model can only be used as a reference to calibrate the post-injection strategy. Of course, the calibration should be in the side of security and estimated ξ should be higher than δ_{AD}.

4.1.1. ***DOC behaviour with post-injection pulses***

Figure 11 shows two different pulses of post-injection being oxidized inside the DOC. Upper and lower plots are pulses of the same flow in mg/str of post injected fuel at different exhaust mass flows. The test at the upper plot is performed at 0.02 kg/s of exhaust mass flow, whilst the test at the lower plot is performed at 0.08 kg/s. In the left-hand plots, the post-injection is represented together with the response of the CO_2 measured by the Cambustion gas analyser. The measurement from the Cambustion NDIR 500 represents the resultant oxygen consumed by the different oxidised species, such as HC, CO and NO. In the right-hand plots, the measurement of the different temperature sensors is represented. Three dashed lines represent the measured temperature in the DOC core at different axial locations, whilst the continuous lines represent the inlet and outlet temperatures.

As the post-injection pulse is performed during steady state conditions, a peak of CO_2 can be observed. This peak is shown almost at the same time of the post-injection event, therefore it means that the oxidation of the fuel is done at the same moment for both exhaust mass flows. It does not happen the same with temperature; when observing temperature plots, they show an important relation between the delay and the exhaust mass flow. The test with the lowest exhaust mass flow, which in this case is the upper plot, shows a notable delay with respect to the other test. What is more, it can be seen in both figures how the axial temperature at the core of the DOC is being passed from one section to the following, just like a wave of energy transmitted by the flow. Thus, the portion of exhaust flow with the CO_2 peak comes out of the DOC at the temperature of the last section of the DOC, which is at the temperature of the steady state conditions. It can be also seen how the temperature decreases inside the DOC due to doc thermal inertia and heat transmission effects with the surroundings, since the DOC is not an isolated system. The peak of the outlet sensor is noticeably lower than that inside the DOC due to mainly two reasons. On the one hand, it is due to heat transmission effects, since it is placed after the last slice of the DOC. On the other hand, it is due to the rather slowness of the NTC sensor in comparison with a fast thermocouple.

4.1.2. ***Steady state pulse model***

In this part of the article, a normalization of the pulse of temperature is done in order to estimate ξ. Experimental tests have been carried out in order to evaluate the behaviour of the pulse under different injection profiles and exhaust mass flows. Tests consist of a train of 5 pulses, as shown in Figure 12, at 6 different air mass flows, as shown in Figure 13, and 3 different post-injection rates: 4, 6 and 8 mg/str. In total, 90 samples of pulses of different characteristics have been performed. An example of the DOC inlet and outlet temperatures, for a given test, is shown in Figure 14. The small temperature peak at the inlet is due to small burning of the post-injection inside the combustion chamber during the last stages of the exhaust stroke.

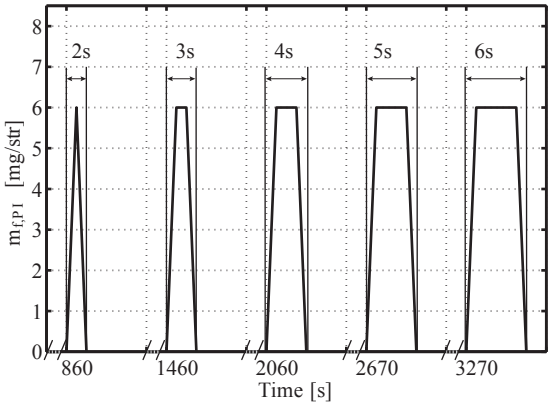

Fig. 12. Shape of the 6 mg/str post-injection at a given air mass flow step.

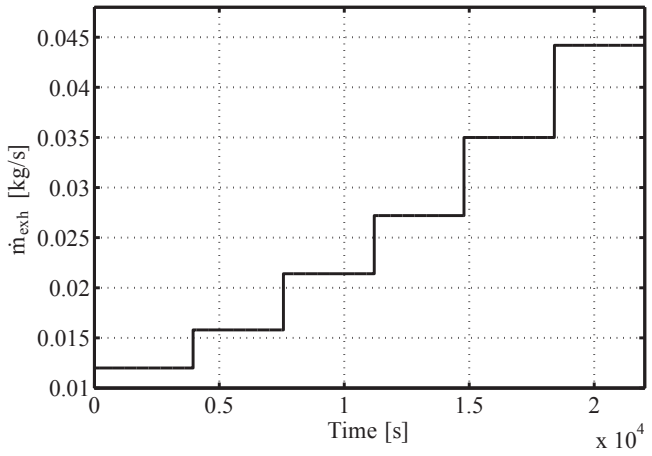

Fig. 13. Air mass flow of the post-injection pulses test.

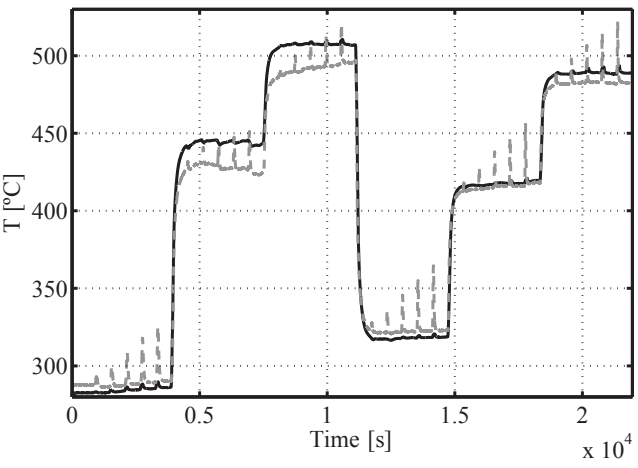

Fig. 14. Inlet (black) and outlet(grey) temperatures at the post-injection pulses test of 6 mg/str.

In equation 2, the normalization of the temperature pulse under steady state conditions is described. The energy released by the oxidation of the pulse in the DOC is the en-

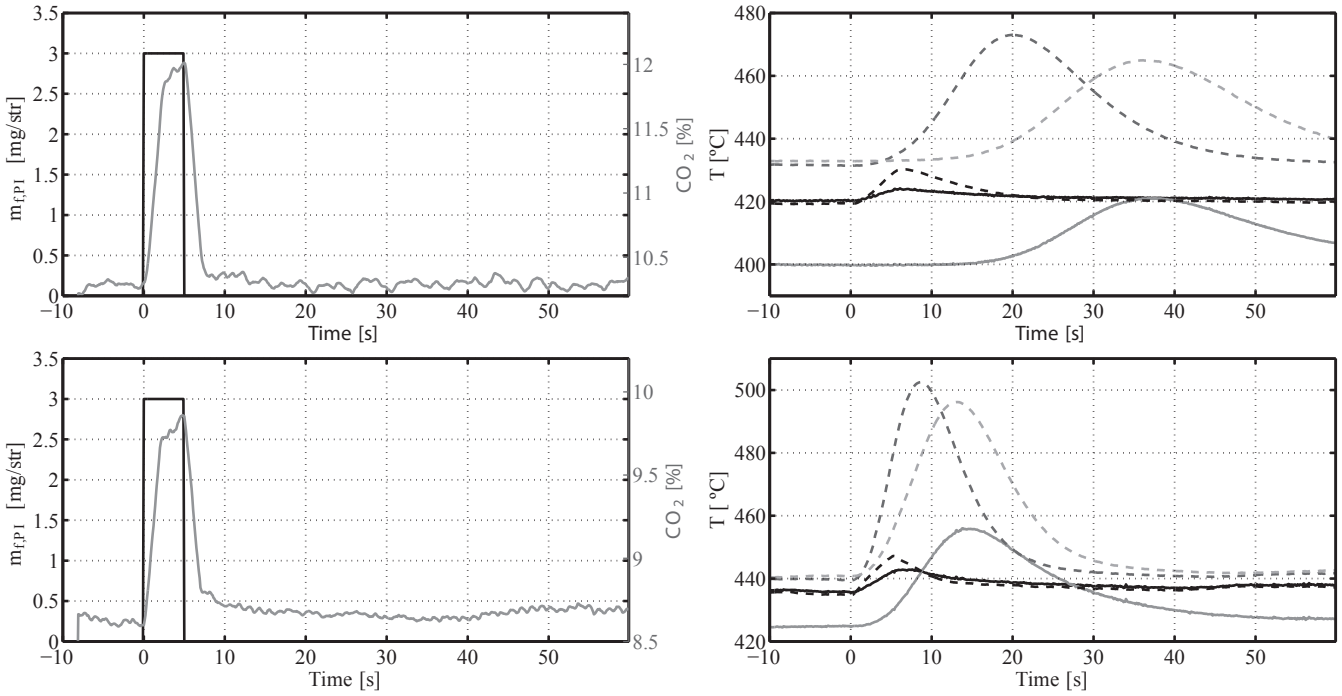

Fig. 11. Insight into the oxidation of a pulse of post injected fuel for a mass flow of 0.02 kg/s (Top plots) and 0.08 kg/s (Bottom plots). Right legend: inlet temperature (black), outlet temperature (grey), intermediate temperature 1 (dashed black), intermediate temperature 2 (dashed dark grey) and intermediate temperature 3 (dashed light grey).

ergy used to increase the temperature of the air during the pulse:

$$\int \dot{m}_{f,pi} H_f dt = \int \dot{m}_{exh} c_p \frac{\Delta T}{dt} dt \tag{2}$$

where $\dot{m}_{pi}$ is the mass flow of post injected fuel, H_f is the lower heating value of the fuel, c_p is the specific heat capacity of the air, ΔT is ξ and $\dot{m}_{exh}$ is the exhaust mass flow. $\dot{m}_{exh}$ is calculated through the addition of the air mass flow and the fuel mass flow.

After integrating the mass of post injected fuel and, whilst keeping constant the air mass flow and keeping the integral of the temperature pulse:

$$m_{f,pi} H_f = \dot{m}_{exh} c_p \int \Delta T \tag{3}$$

A linear correlation is eventually obtained:

$$\int \Delta T = \frac{m_{f,pi}}{\dot{m}_{exh}} \frac{H_f}{c_p} \tag{4}$$

where H_f/c_p is constant and therefore $m_{f,pi}/\dot{m}_{exh}$ and $\int \Delta T$ are correlated with a polynomial function of grade 1 with origin in 0 and slope H_f/c_p, as shown in Figure 15. Despite dispersion can be appreciated, which may be due to inaccuracies in the ECU calculations of post-injected fuel and heat transmission effects, a linear increasing tendency is appreciated as $m_{f,pi}/\dot{m}_{exh}$ increases.

One pulse of temperature has been taken as a reference vector ΔT_{pulse}, *i.e.* a model (Fig. 16), whilst the rest of

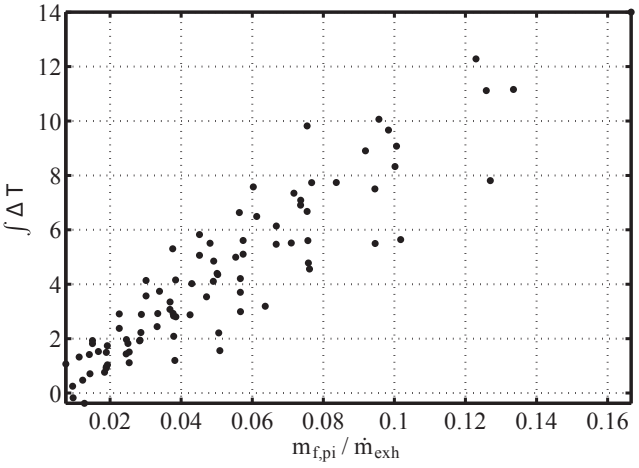

Fig. 15. Linear correlation between the integral of the temperature pulse and the fraction of post-injection mass over air mass flow.

the pulses at different conditions can be estimated through a convolution process (eq. 5). The convolution equation 5 combines the temperature pulse vector model with the post-injection profile p, which is defined by injection duration and rate.

$$\Delta T_{pulse} = p * \Delta T_m = \sum_{i=1}^{n} p[i] \Delta T_m[n - i + 1] \tag{5}$$

where n is the length of the post-injection vector p.

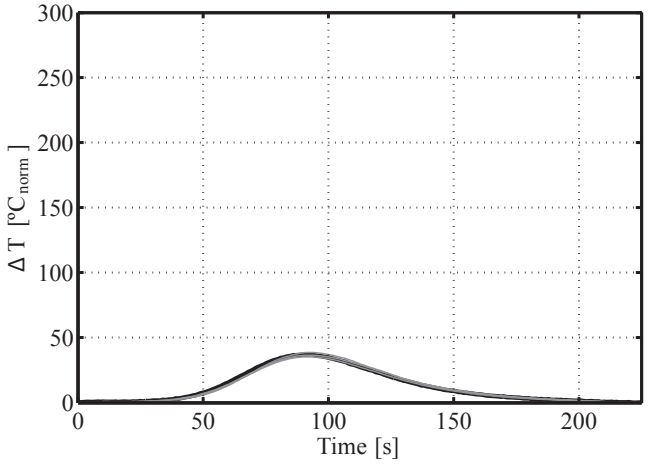

Fig. 16. Black: Reference vector model at 0.016g/s, 0.3s injection and 6 mg/str. Grey: normalised temperatures increment at 0.016 g/s and 0.3s injection for 4, 8 and 10 mg/str.

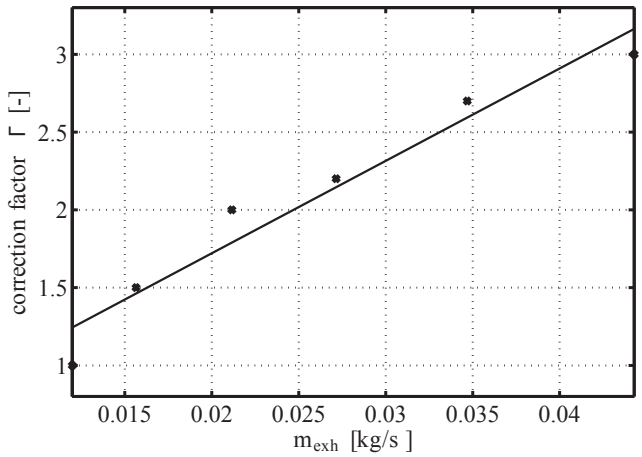

Fig. 17. Correction factor for the pulse duration and the normalised temperature pulse.

The duration of the temperature pulse (eq. 6), as well as the peak temperature (eq. 7), have to be resized by a correction factor Γ, which depends on the air mass flow. This factor, fitted for the previously mentioned tests, describes a linear correlation, as shown in Figure 17. Since the correction factor keeps constant the area of the normalised temperature pulse, energy is conserved.

$$t_{pulse,corr} = \frac{t_{pulse}}{\Gamma} \tag{6}$$

$$\Delta T_{pulse,corr} = \Delta T_{pulse}\Gamma \tag{7}$$

Where t_{pulse} is the pulse duration and ΔT_{pulse} is the normalised temperature increment of the pulse.

It can be observed in Figure 18 the results of the application of the temperature normalization to pulse tests with 4, 6 and 8 mg/str at 0.044 g/s. Although the model is not completely able to reproduce temperature dynamics, ξ_{max} is well captured. As shown in Figure 19, the model can be used to calibrate the strategy with a map of ΔT_{max} depending on air mass flow.

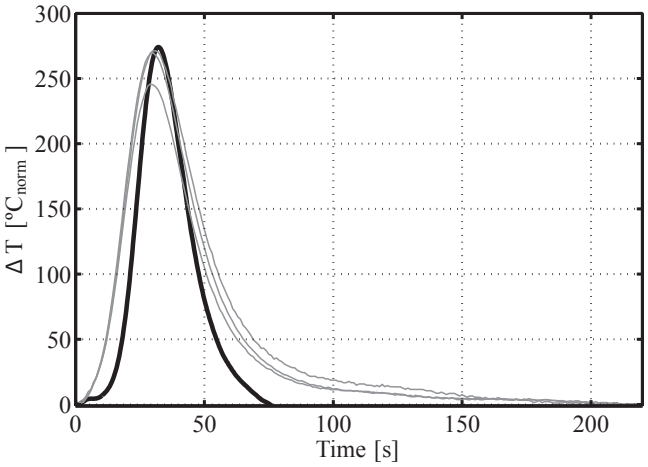

Fig. 18. Black: Modelled temperature increment at 0.044 g/s and 0.6s injection. Grey: experimental normalised temperature at 0.044 g/s and 0.6s injection.

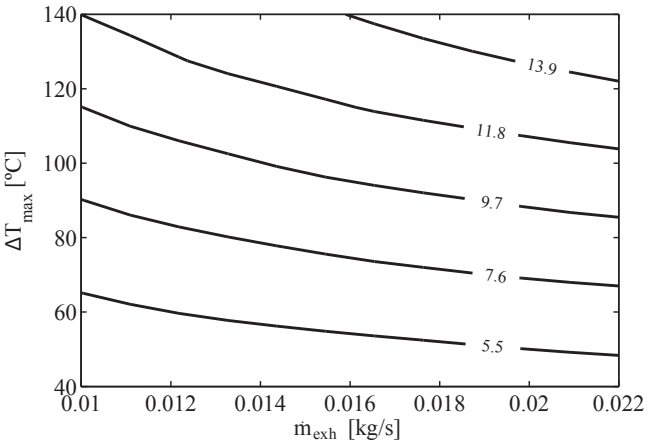

Fig. 19. Modelled post-injection duration (seconds) to generate a pulse with ΔT_{max} depending on air mass flow. Injection rate is 8 mg/str.

4.2. *Application to active diagnostics*

Figure 21 shows active diagnostics for the nominal catalyst during a NEDC cycle in which post-injections have been applied. During the urban phase, small oxidation intervals may be appreciated due to the oxidation of accumulated engine-raw HC emissions, while the inlet temperature overcomes the activation temperature. This phenomena can be also appreciated in Figure 8 during passive diagnosis, due to the fact that post-injections have not been applied yet. When the cycle comes to the extra-urban phase, the DOC temperature rises above the light-off and two post-injections are applied. Both post-injections have 8 mg/str rate. The first post-injection has 7 seconds duration and the second post-injection has 3 seconds duration. Although the fuel signal might have accuracy errors, the model does not predict temperature increments, so post-injection events are set to provide sufficient temperature increase.

The first post-injection shows how enough post-injected

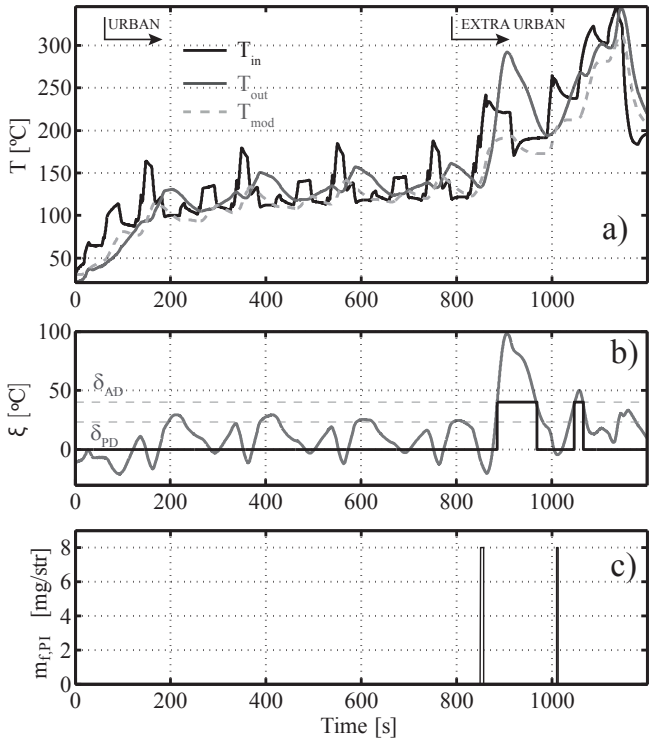

Fig. 20. Active diagnostics with the nominal catalyst during a NEDC test. a) Temperatures b) Grey: ξ. Black: 0 when no oxidation and δ_{AD} when $\xi > \delta_{AD}$. c) Post-injection.

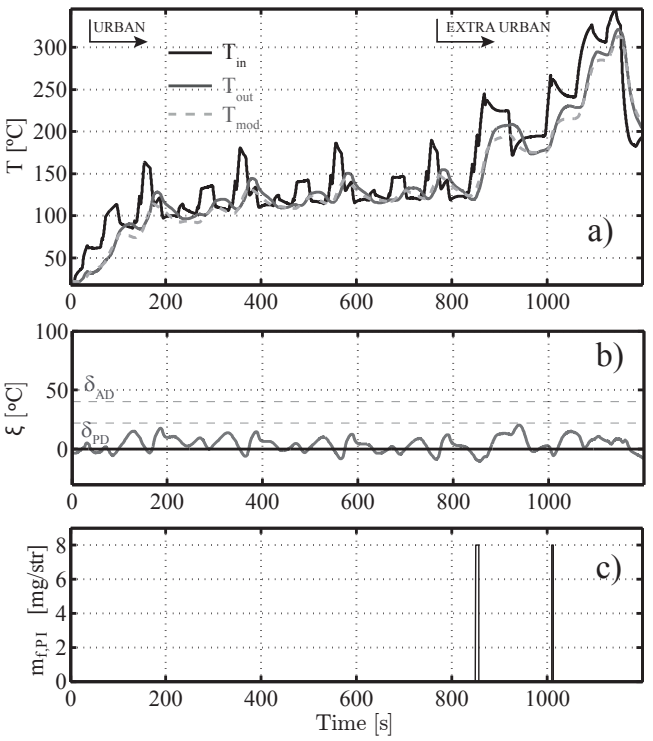

Fig. 21. Active diagnostics with the non-impregnated catalyst during a NEDC test. a) Temperatures b) Grey: ξ. Black: 0 when no oxidation and δ_{AD} when $\xi > \delta_{AD}$. c) Post-injection.

fuel during normal engine operation can rise ξ until a maximum value of 100°C, which ensures a proper diagnostics. Thus, in this case, when active diagnostics is enabled, the applied post-injections increase sufficiently $\xi > \delta_{AD}$ and there is a high check that the DOC is working properly.

By contrast, results of active diagnostics are shown for the non-impregnated DOC, also during a NEDC in Figure 21, in which the same post-injections have been virtually applied. In this case, during the temporal window opened after the post-injections, the residuum ξ does not overcome in any case neither δ_{PD} nor δ_{AD} so according to the diagnostics strategy shown in Figure 3, the result is negative and the DOC is not able to oxidise.

5. Conclusions

The article presents a diagnostics strategy for diesel oxidation catalysts based on the exothermic reaction generated by the oxidable species from the engine raw emissions such as HC, CO and NO, but also on the exothermic reaction generated by fuel post-injections. The diagnosis algorithm presented is able to discern whether a DOC is able to oxidise or not. A passive DOC model, based on a non-impregnated DOC, is used and its accuracy is argued for diagnosis purposes. The simplicity of the model allows to use it in ECU environment.

Two thresholds of temperature increment, one lower and other higher, are set in order to evaluate the DOC state. Passive diagnosis uses the low threshold, set by the model accuracy, to have a low check. The high threshold is set to ensure 100% the state of the DOC: when post-injections are performed and the residuum overcomes the high threshold, the DOC is able to oxidise, but when the residuum do not overcome the low threshold, the DOC is not able to oxidise and becomes faulty.

A deep analysis of the behaviour of post-injection pulses under steady state conditions has been carried out. A model of the pulses has been developed and it can be used to estimate ξ and calibrate the strategy.

6. Acknowledgements

This research has been partially financed by the Spanish Ministerio de Economía y Competitividad, through project TRA2013-40853-R 'Desarrollo de nuevas técnicas de limitación de la pérdida de presión en DPFs para reducir las emisiones y el consumo de los motores diesel (PRELIMIT)'.

References

[1] B. Daham, H. Li, G. Andrews, K. Ropkins, J. Tate, M. Bell, Comparison of real world emissions in urban driving for EURO 1-4 vehicles using a PEMS .

[2] U. G. Alkemade, B. Schumann, Engines and exhaust after treatment systems for future automotive appli-

cations, Solid State Ionics 177 (26-32) (2006) 2291 – 2296.

[3] G. Vitale, P. Siebenbrunner, H. Halser, J. Bachler, U. Pfahl, OBD Algorithms: Model-based Development and Calibration, in: SAE Technical Paper, SAE International, 2007.

[4] T. V. Johnson, Review of Diesel Emissions and Control, SAE Int. J. Fuels Lubr. (2010) 16–29.

[5] Y.-D. Kim, W.-S. Kim, Re-evaluation and Modeling of a Commercial Diesel Oxidation Catalyst, Industrial & Engineering Chemistry Research 48 (14) (2009) 6579–6590.

[6] S. Bai, J. Tang, G. Wang, G. Li, Soot loading estimation model and passive regeneration characteristics of DPF system for heavy-duty engine, Applied Thermal Engineering 100 (2016) 1292–1298.

[7] A. Frobert, Y. Creff, O. Lepreux, L. Schmidt, S. Raux, Generating Thermal Conditions to Regenerate a DPF: Impact of the Reductant on the Performances of Diesel Oxidation Catalysts, in: SAE Technical Paper, SAE International, 2009.

[8] S. Stadlbauer, H. Waschl, A. Schilling, L. del Re, DOC Temperature Control for Low Temperature Operating Ranges with Post and Main Injection Actuation, in: SAE Technical Paper, SAE International, 2013.

[9] B. Guan, R. Zhan, H. Lin, Z. Huang, Review of state of the art technologies of selective catalytic reduction of NOx from diesel engine exhaust, Applied Thermal Engineering 66 (1) (2014) 395–414.

[10] J. Li, T. Szailer, A. Watts, N. Currier, A. Yezerets, Investigation of the Impact of Real-World Aging on Diesel Oxidation Catalysts, SAE Int. J. Engines 5 (2012) 985–994.

[11] R. Schultz, P. H. Meckl, Light-Off Temperature Shift for Catalyzed Diesel Particulate Filter On-Board Diagnostics, in: SAE Technical Paper, SAE International, 2012.

[12] M. H. Wiebenga, C. H. Kim, S. J. Schmieg, S. H. Oh, D. B. Brown, D. H. Kim, J.-H. Lee, C. H. Peden, Deactivation mechanisms of Pt/Pd-based diesel oxidation catalysts, Catalysis Today 184 (1) (2012) 197 – 204, catalytic Control of Lean-Burn Engine Exhaust Emissions.

[13] E. Zervas, Impact of different configurations of a Diesel oxidation catalyst on the CO and HC tail-pipe emissions of a Euro4 passenger car, Applied Thermal Engineering 28 (8) (2008) 962–966.

[14] C. Guardiola, B. Pla, J. Mora, D. Lefebvre, Control Oriented Model for Diesel Oxidation Catalyst Diagnosis, IFAC-PapersOnLine 48 (15) (2015) 427 – 433.

[15] M. van Nieuwstadt, D. Upadhyay, F. Yuan, Diagnostics for Diesel Oxidation Catalysts, in: SAE Technical Paper, SAE International, 2005.

[16] O. Lepreux, Y. Creff, N. Petit, Warm-up strategy for a Diesel Oxidation Catalyst, in: Control Conference (ECC), 2009 European, 3821–3826, 2009.

[17] K. Yamamoto, K. Takada, J. Kusaka, Y. Kanno, M. Nagata, Influence of Diesel Post Injection Timing on HC Emissions and Catalytic Oxidation Performance, in: SAE Technical Paper, SAE International, 2006.

[18] A. Russell, W. S. Epling, Diesel Oxidation Catalysts, Catalysis Reviews 53 (4) (2011) 337–423.

[19] C. S. Sampara, E. J. Bissett, D. Assanis, Hydrocarbon storage modeling for diesel oxidation catalysts, Chemical Engineering Science 63.

[20] P. Chen, J. Wang, Control-oriented modeling of thermal behaviors for a Diesel oxidation catalyst, in: American Control Conference (ACC), 2012, 4987–4992, 2012.

[21] M. Zheng, S. Banerjee, Diesel oxidation catalyst and particulate filter modeling in active Flow configurations, Applied Thermal Engineering 29 (14-15) (2009) 3021 – 3035.

[22] O. Lepreux, Y. Creff, N. Petit, Model-based temperature control of a diesel oxidation catalyst, Journal of Process Control 22 (1) (2012) 41 – 50.

[23] A. Boatas, M. A. Dillies-Peltier, B. Dubuisson, OBD Using Statistical Pattern Recognition, in: SAE Technical Paper, SAE International, 2000.

[24] S. Ye, Y. H. Yap, S. T. Kolaczkowski, K. Robinson, D. Lukyanov, Catalyst light-off experiments on a diesel oxidation catalyst connected to a diesel engine-methodology and techniques, Chemical Engineering Research and Design 90 (6) (2012) 834 – 845.

[25] G. J. Bartley, Identifying Limiters to Low Temperature Catalyst Activity, in: SAE Technical Paper, SAE International, 2015.

[26] E. Zervas, Development of an indicator for the emission control of diesel passenger cars, Applied Thermal Engineering 28 (11) (2008) 1437–1442.

[27] Y.-W. Kim, M. V. Nieuwstadt, G. Stewart, J. Pekar, Model Predictive Control of DOC Temperature during DPF Regeneration, in: SAE Technical Paper, SAE International, 2014.